Electronic Supplementary Material (ESI) for Nanoscale.
This journal is © The Royal Society of Chemistry 2017

Control on photo-responsive assembly of a stilbene-containing amphiphile by using pillar[5]arene-based host−guest interactions

Huangtianzhi Zhu, Liqing Shangguan, Danyu Xia, Julfikar Hassan Mondal and Bingbing Shi*

Department of Chemistry, Zhejiang University, Hangzhou,

Zhejiang 310027, P. R. China

Fax and Tel: +86-571-8795-3189; Email address: bingbingshi@zju.edu.cn

Electronic Supplementary Information (11 pages)

1. Materials and methods

All reagents were commercially available and used as supplied without further purification. The water-soluble pillar[5]arene was synthesized according to a published procedure.[S1] ^{1}H or ^{13}C NMR spectra were recorded with a Bruker Avance DMX 400 spectrophotometer with use of the deuterated solvent as the lock and the residual solvent or TMS as the internal reference. High-resolution mass spectrometry experiments were performed with a Bruker 7-Tesla FT-ICR mass spectrometer equipped with an electrospray source (Billerica, MA, USA). The melting points were collected on a SHPSIC WRS-2 automatic melting point apparatus. UV-vis spectra were taken on a Perkin-Elmer Lambda 35 UV−vis spectrophotometer. The determination of the critical aggregation concentration (CAC) values was carried out on a DDS-307 instrument. Scanning electron microscopy investigation was carried out on a JEOL 6390LV instrument. Transmission electron microscopy investigations were carried out on a JEM-1200EX instrument. Dynamic light scattering was carried out on a Malvern Nanosizer S instrument at room temperature.

2. Synthesis and characterizations of compounds

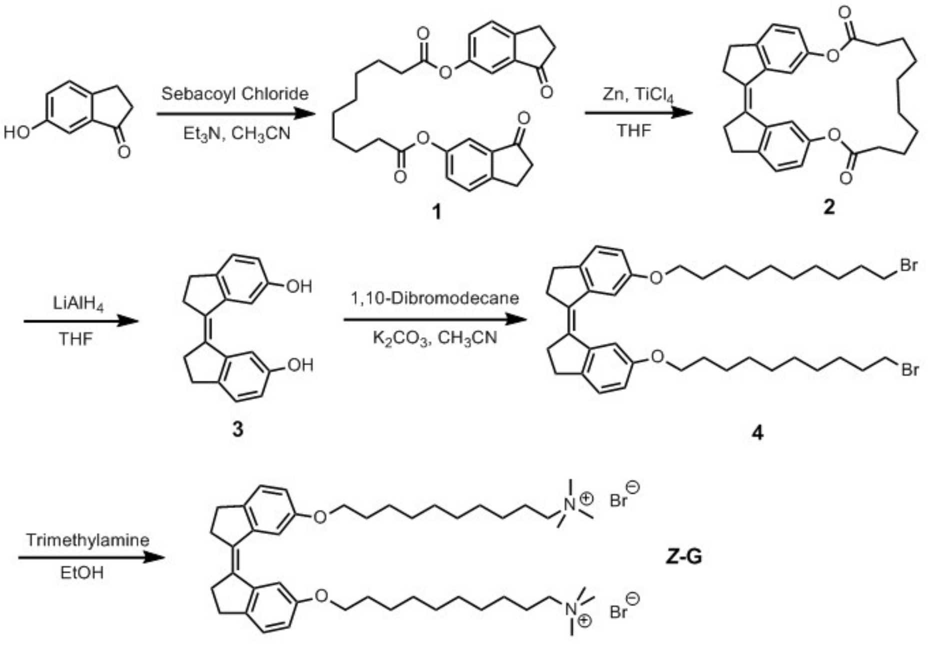

Compound **1**: To a solution of 6-methyl-1-indanone (3.00 g, 20.3 mmol) and Et$_3$N (3.30 mL, 24.0 mmol) in 50.0 mL of CH$_3$CN was added sebacoyl chloride (2.61 g, 10.8 mmol), the mixture was stirred overnight. After cooling to room temperature, undissolved solid was filtered. The filtrate was concentrated under reduced pressure to obtain the crude product, which was purified by column chromatography using hexane : ethylacetate = 2 : 1 as the eluent to give pure product as a white solid (4.00 g, 85.5%), mp 176.2−178.0 °C. ^{1}H NMR (400 MHz, CDCl$_3$, 298 K) δ (ppm): 7.48 (d, J = 8.2 Hz, 2H), 7.44 (s, 2H), 7.30 (d, J = 10.5 Hz, 2H), 3.12 (t, 4H), 2.75 (t, 4H), 2.58 (t, J = 7.5 Hz, 4H), 1.81–1.72 (m, 4H), 1.42 (m, J = 10.5 Hz, 8H). ^{13}C NMR (100 MHz, CDCl$_3$, 298K) δ (ppm): 206.01, 172.21, 152.26, 150.18, 138.34, 128.42, 127.49, 116.39, 36.86, 34.27, 29.02, 25.46, 24.86. HRMS: *m/z* calcd for [M + Na]$^+$ C$_{28}$H$_{30}$O$_6$Na$^+$, 485.1935, found 485.1921, error –2.9 ppm.

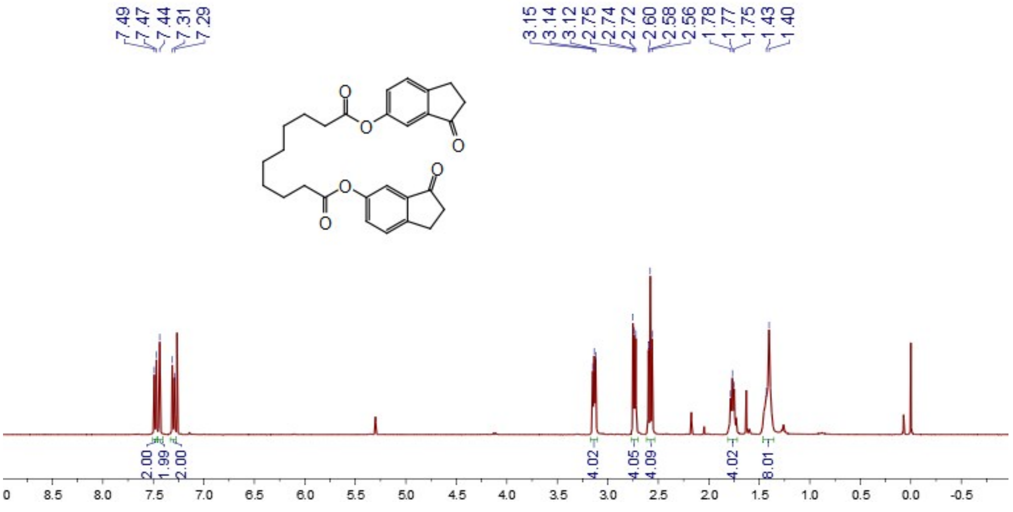

Fig. S1 ^{1}H NMR spectrum (400 MHz, CDCl$_3$, 298 K) of compound **1**.

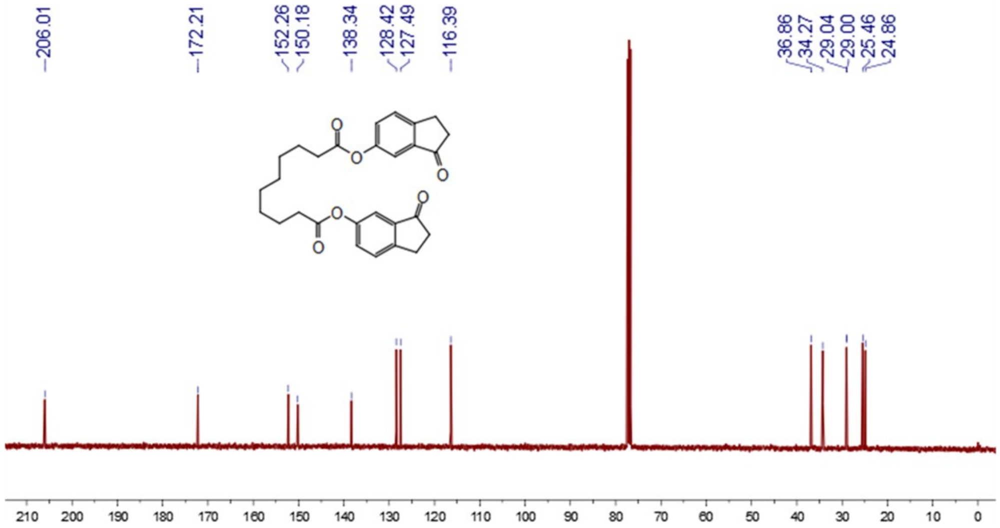

Fig. S2 ^{13}C NMR spectrum (100 MHz, $CDCl_3$, 298 K) of compound **1**.

Compound **2**: $TiCl_4$ (5.50 mL, 50.7 mmol) was added carefully to a suspension of zinc powder (6.48 g, 101 mmol) in 250 mL of THF and then refluxed for 1 h. A solution of compound **1** (3.50 g, 7.57 mmol) in 200 mL of THF was injected into the reaction mixture dropwise and reacted overnight. After cooling to room temperature, the reaction was quenched with saturated NH_4Cl aqueous and stirred for 1 h. The organic layer was concentrated under reduced pressure to obtained crude product, which was used in the next step without further purification.

Compound **3**: To a solution of crude compound **2** (3.00 g) in 250 mL of dry THF was added excess $LiAlH_4$. After the mixture was stable, it was heated to reflux overnight. 10.0 mL of water was added carefully to quench the reaction. Solvents were removed on a rotary evaporator to obtain crude product which was used in the next step without further purification.

Compound **4**: Crude compound **3** (0.300 g), 1.10-dibromodecane (3.00 g, 10.0 mmol) and K_2CO_3 (2.00g, 14.6 mmol) were mixed in 30.0 mL of CH_3CN and refluxed overnight. After cooling to room temperature, undissolved solid was filtered. The filtrate was concentrated to obtain the crude product, and then purified by column chromatography using hexane : dichloromethane = 3 : 1 as the eluent to give pure compound **4** as a white solid (0.392 g). ^{1}H NMR (400 MHz, $CDCl_3$, 298 K) δ (ppm): 7.64 (d, J = 2.0 Hz, 2H), 7.17 (d, J = 8.2 Hz, 2H), 6.74 (d, J = 10.4 Hz, 2H), 3.90 (t, J = 6.4 Hz, 4H), 3.40 (t, J = 6.9 Hz, 4H), 2.95–2.88 (m, 4H), 2.81 (t, J = 6.4 Hz, 4H), 1.90–1.78 (m, 4H), 1.76–1.68 (m, 4H), 1.41 (d, J = 6.7 Hz, 8H), 1.29 (s, 16H). ^{13}C NMR (100 MHz, $CDCl_3$, 298K) δ (ppm): 157.51, 141.60, 140.50, 135.41, 125.54, 114.79, 108.98, 68.23, 35.42, 34.06, 32.85, 29.87, 29.52, 29.46, 29.42, 29.39, 28.80, 28.20, 26.16.

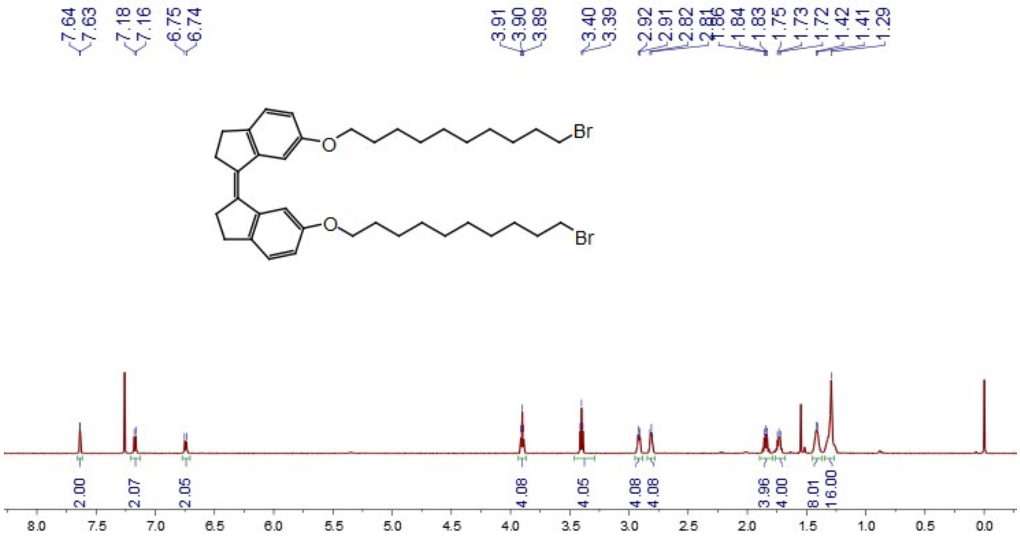

Fig. S3 ^{1}H NMR spectrum (400 MHz, $CDCl_3$, 298 K) of compound **4**.

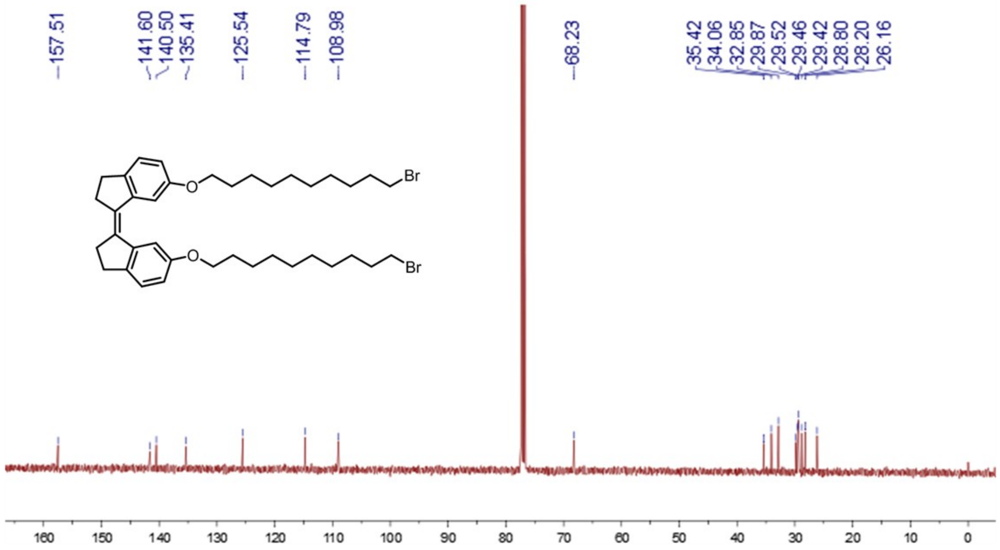

Fig. S4 ^{13}C NMR spectrum (100 MHz, $CDCl_3$, 298 K) of compound **4**.

Compound ***Z*-G**: Compound **4** (0.200 g, 0.286 mmol) was dissolved in 60.0 mL of EtOH and 3.00 mL of a solution of trimethylamine in MeOH. The reaction mixture was refluxed overnight. All solvents were removed on a rotary evaporator to obtain pure compound ***Z*-G** as a white solid (0.233 g, 99%), mp 146.2−147.5 °C. ^{1}H NMR (400 MHz, DMSO-d_6, 298 K) δ (ppm): 7.48 (d, J = 2.0 Hz, 2H), 7.23 (d, J = 8.3 Hz, 2H), 6.79 (d, J = 10.4 Hz, 2H), 3.90 (t, J = 6.3 Hz, 4H), 3.29–3.23 (m, 4H), 3.04 (s, 18H), 2.87 (d, J = 6.3 Hz, 4H), 2.77 (s, 4H), 1.68 (d, J = 7.7 Hz, 8H), 1.28 (s, 16H). ^{13}C NMR (100 MHz, DMSO-d_6, 298 K) δ (ppm): 156.90, 140.83, 140.19, 135.01, 125.89, 114.57, 108.49, 67.59, 65.21, 52.10, 34.81, 29.21, 28.96, 28.80, 28.54, 25.77, 25.61, 22.05. HRMS: m/z calcd for $[M - 2Br]^{2+}$, $C_{44}H_{72}N_2O_2^{2+}$, 330.2791, found 330.2761, error −9.1 ppm.

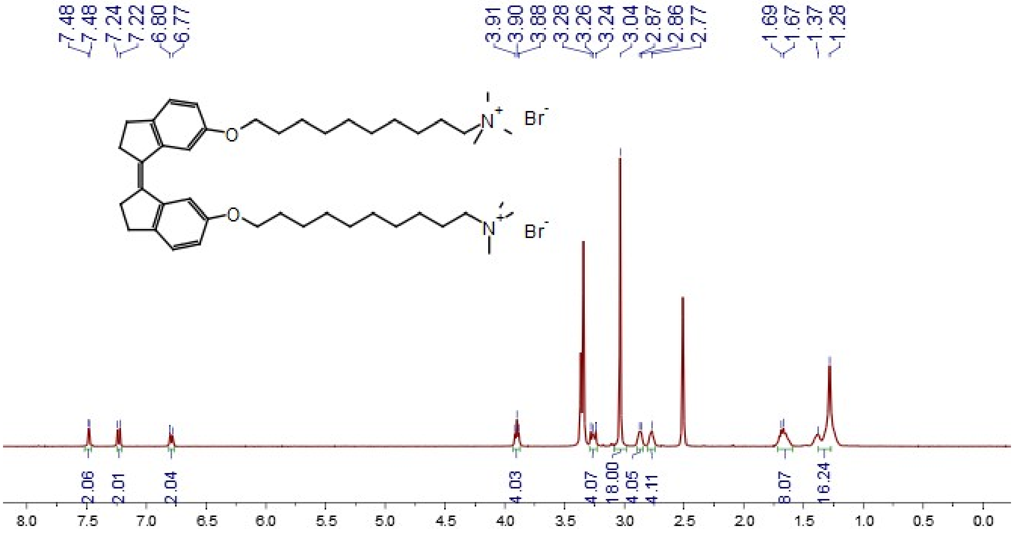

Fig. S5 ^{1}H NMR spectrum (400 MHz, DMSO-d_6, 298 K) of compound ***Z*-G**.

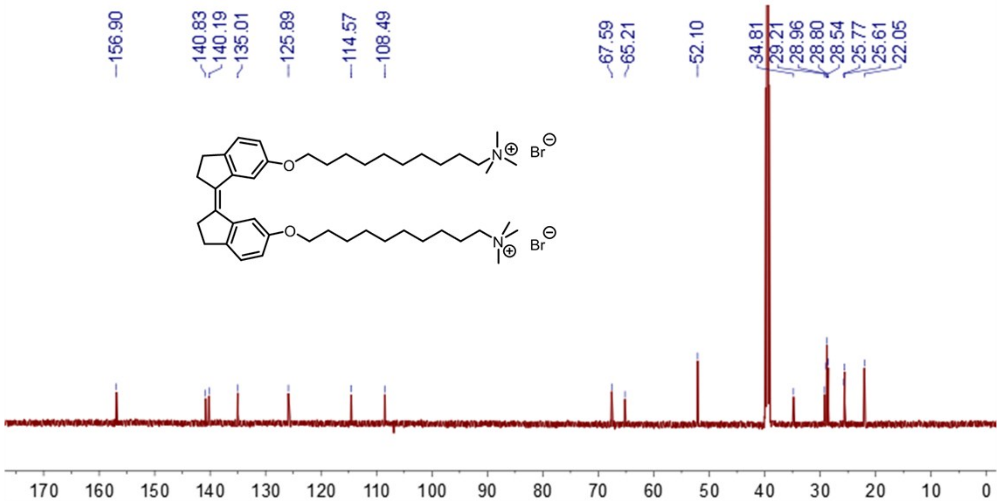

Fig. S6 ^{13}C NMR spectrum (100 MHz, DMSO-d_6, 298 K) of compound ***Z*-G**

3. *Studies of photoisomerization of **Z-G***

^{1}H NMR spectra

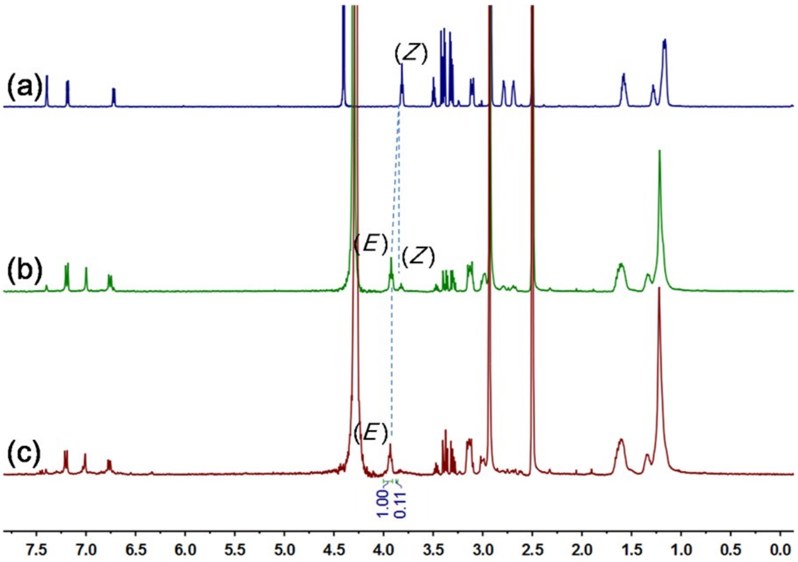

Fig. S7 ^{1}H NMR spectra (400 MHz, DMSO-d_6 : D_2O = 1 : 1, 298K): (a) ***Z*-G** (1.00 mM); (b) (a) after irradiation at 387 nm for 6 h; (c) (a) after irradiation at 387 nm for 10 h. The mixture contains ***E*-G** (90.1%) and ***Z*-G** (9.90%) determined by integral areas.

UV-vis spectra

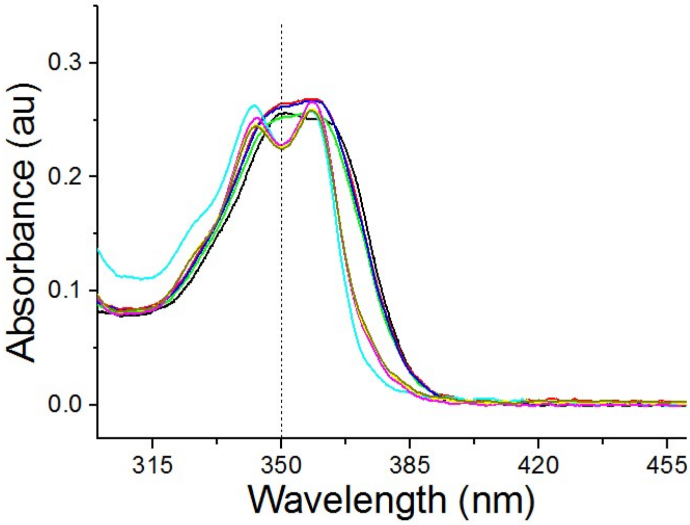

Fig. S8 UV−vis spectra of a solution of ***Z*-G** (0.0100 mM in DMSO : H_2O = 1 : 1) upon alternating irradiation at 387 nm for 10 h and 360 nm for 8 h. Absorption intensity at 350 nm was used to construct cyclic changing curve.

High concentration ^1H NMR spectra

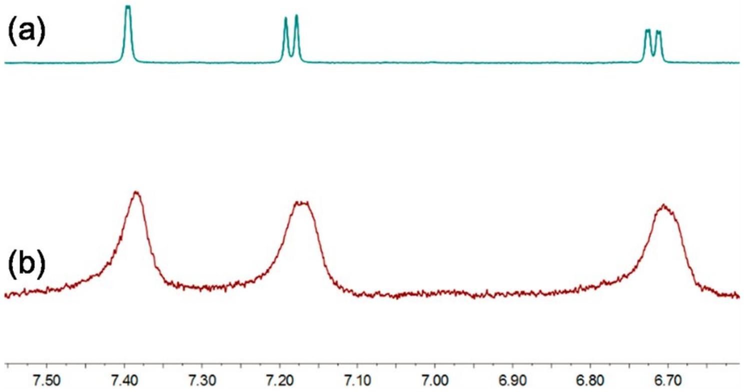

Fig. S9 Partial ^{1}H NMR spectra (400 MHz, DMSO-d_6 : D_2O = 1 : 1, 298K) : (a) ***Z*-G** (1.00 mM); (b) ***Z*-G** (~15.00 mM). The peaks became broad slightly shifted upfield, verifying the π–π interactions between ***Z*-G**.

*4. Isothermal Titration Calorimetry (ITC) of **WP5** and **Z-G***

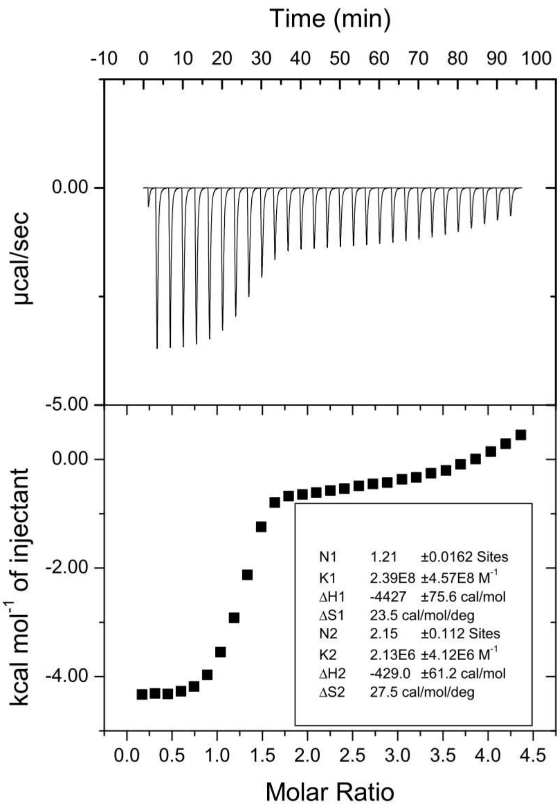

Fig. S10 Isothermal Titration Calorimetry (ITC) of **WP5** (2.00 mM) and ***Z*-G** (0.100 mM) in water at 298 K. (Top) Raw ITC data. (Bottom) Net reaction heat obtained from the integration of the calorimetric traces. From the data, the ratio between **WP5** and ***Z*-G** is 2.15.

*5. NOESY NMR spectrum of **WP5⊃Z-G***

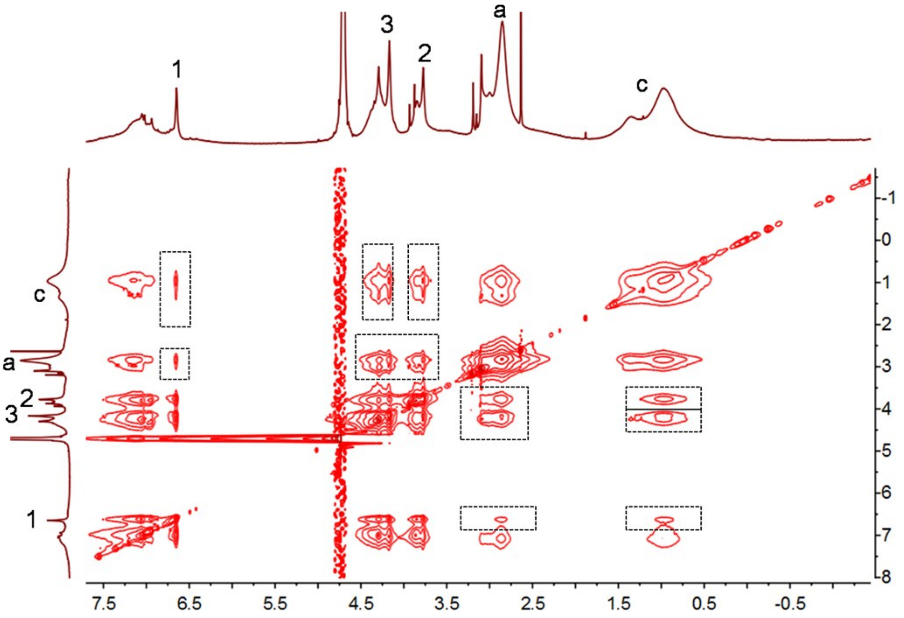

Fig. S11 NOESY NMR spectrum (400 MHz, D_2O, 298K) of a mixture of **WP5** (2.00 mM) and ***Z*-G** (1.00 mM). NOE correlation signals between host and guest are marked.

6. Determination of critical aggregation concentration (CAC)

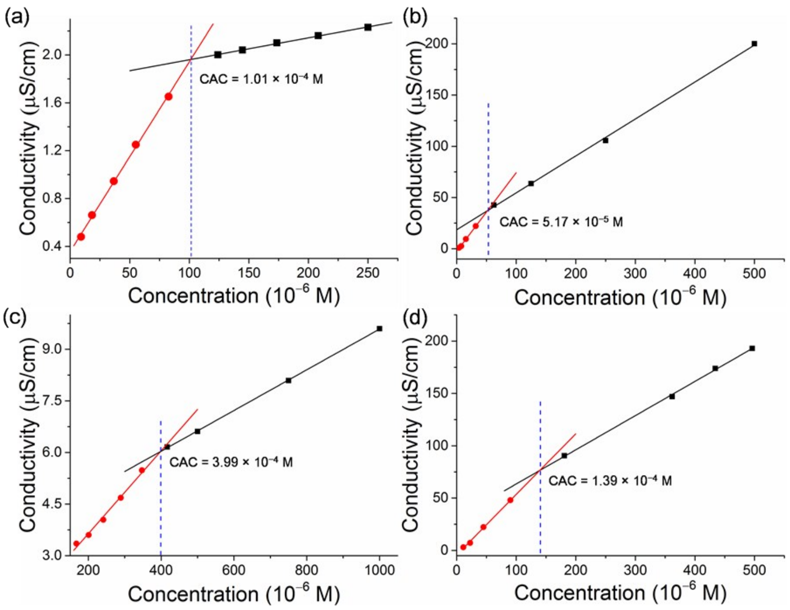

Fig. S12 The concentration-dependent conductivity of (a) ***Z*-G**, (b) **WP5⊃*Z*-G**, (c) ***E*-G** and (d) **WP5⊃*E*-G**. The critical aggregation concentration of each amphiphilic system is shown in figures.

*7. Dynamic light scattering (DLS) result of **E-G***

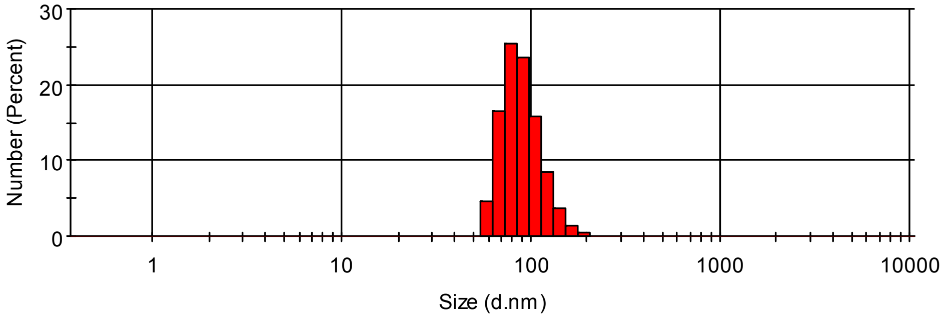

Fig. S13 DLS result of ***E*-G** (~1.00 mM) in water. The average diameter is 90.8 nm.

8. AFM images of self-assembly morphologies

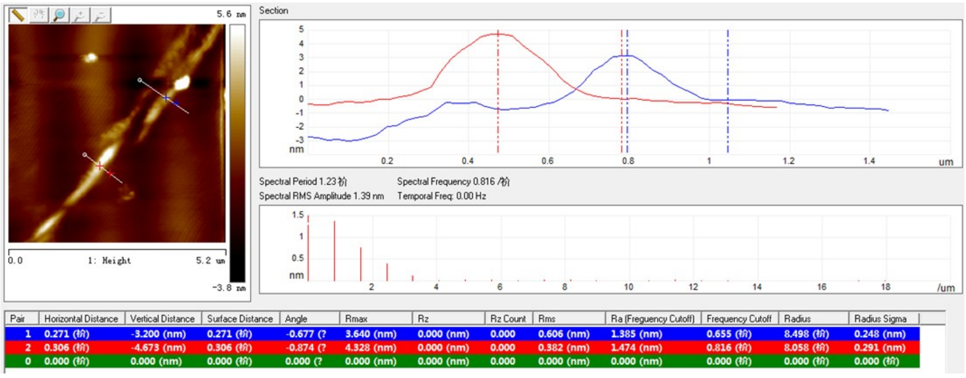

Spectral Period 1.23 祄 Spectral Frequency 0.816 /祄

Spectral RMS Amplitude 1.39 nm Temporal Freq: 0.00 Hz

Pair	Horizontal Distance	Vertical Distance	Surface Distance	Angle	Rmax	Rz	Rz Count	Rms	Ra (Frequency Cutoff)	Frequency Cutoff	Radius	Radius Sigma
1	0.271 (祄)	-3.200 (nm)	0.271 (祄)	-0.677 (?	3.640 (nm)	0.000 (nm)	0.000	0.606 (nm)	1.385 (nm)	0.655 (祄)	8.498 (祄)	0.248 (nm)
2	0.306 (祄)	-4.673 (nm)	0.306 (祄)	-0.874 (?	4.328 (nm)	0.000 (nm)	0.000	0.382 (nm)	1.474 (nm)	0.816 (祄)	8.058 (祄)	0.291 (nm)
0	0.000 (祄)	0.000 (nm)	0.000 (祄)	0.000 (?	0.000 (nm)	0.000 (nm)	0.000	0.000 (nm)	0.000 (nm)	0.000 (祄)	0.000 (祄)	0.000 (祄)

Fig. S14 AFM image of the self-assembled nanoribbons. The thicknesses of these nanoribbons are measured to be 3.20 nm and 4.67 nm, which are about the length of two ***Z*-G** molecules with antiparallel packing.

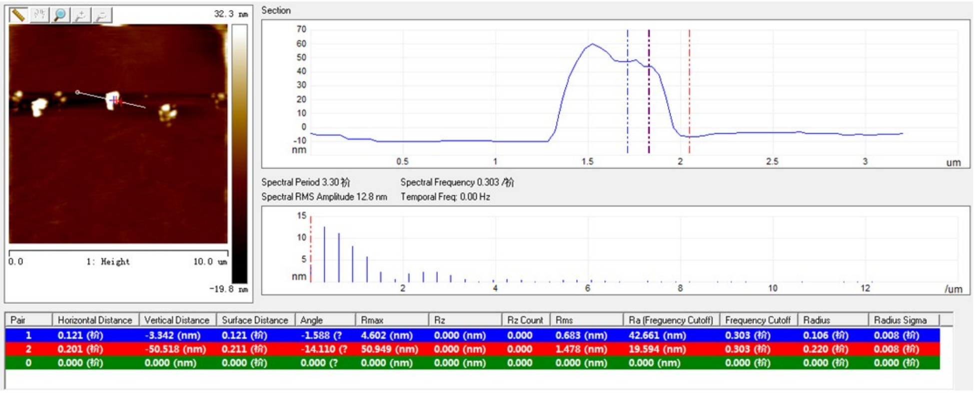

Spectral Period 3.30 祄 Spectral Frequency 0.303 /祄

Spectral RMS Amplitude 12.8 nm Temporal Freq: 0.00 Hz

Pair	Horizontal Distance	Vertical Distance	Surface Distance	Angle	Rmax	Rz	Rz Count	Rms	Ra (Frequency Cutoff)	Frequency Cutoff	Radius	Radius Sigma
1	0.121 (祄)	-3.342 (nm)	0.121 (祄)	-1.588 (?	4.602 (nm)	0.000 (nm)	0.000	0.683 (nm)	42.661 (nm)	0.303 (祄)	0.106 (祄)	0.008 (祄)
2	0.201 (祄)	-50.518 (nm)	0.211 (祄)	-14.110 (?	50.949 (nm)	0.000 (nm)	0.000	1.478 (nm)	19.594 (nm)	0.303 (祄)	0.220 (祄)	0.008 (祄)
0	0.000 (祄)	0.000 (nm)	0.000 (祄)	0.000 (?	0.000 (nm)	0.000 (nm)	0.000	0.000 (nm)	0.000 (nm)	0.000 (祄)	0.000 (祄)	0.000 (祄)

Fig. S15 AFM image of the self-assembled nanocubes. These stacking nanocubes have different thicknesses.

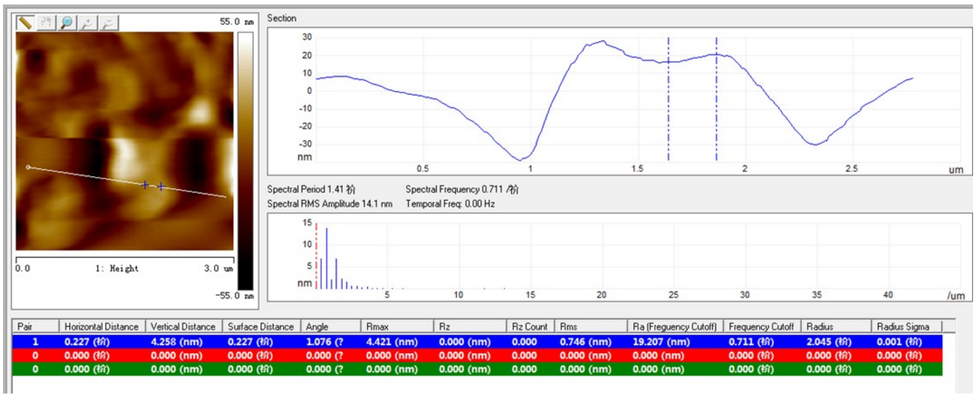

Spectral Period 1.41 祄
Spectral Frequency 0.711 /祄
Spectral RMS Amplitude 14.1 nm
Temporal Freq: 0.00 Hz

Pair	Horizontal Distance	Vertical Distance	Surface Distance	Angle	Rmax	Rz	Rz Count	Rms	Ra (Frequency Cutoff)	Frequency Cutoff	Radius	Radius Sigma
1	0.227 (祄)	4.258 (nm)	0.227 (祄)	1.076 (?	4.421 (nm)	0.000 (nm)	0.000	0.746 (nm)	19.207 (nm)	0.711 (祄)	2.045 (祄)	0.001 (祄)
0	0.000 (祄)	0.000 (nm)	0.000 (祄)	0.000 (?	0.000 (nm)	0.000 (nm)	0.000	0.000 (nm)	0.000 (nm)	0.000 (祄)	0.000 (祄)	0.000 (祄)
0	0.000 (祄)	0.000 (nm)	0.000 (祄)	0.000 (?	0.000 (nm)	0.000 (nm)	0.000	0.000 (nm)	0.000 (nm)	0.000 (祄)	0.000 (祄)	0.000 (祄)

Fig. S16 AFM image of the crumpled film. Due to its unsmooth surface, the thickness of this film is hard to measure accurately. However, 4.26 nm is about the length of one bola-type supra-amphiphilic molecule, indicating the film is single-layer.

9. SEM images of self-assembly morphologies

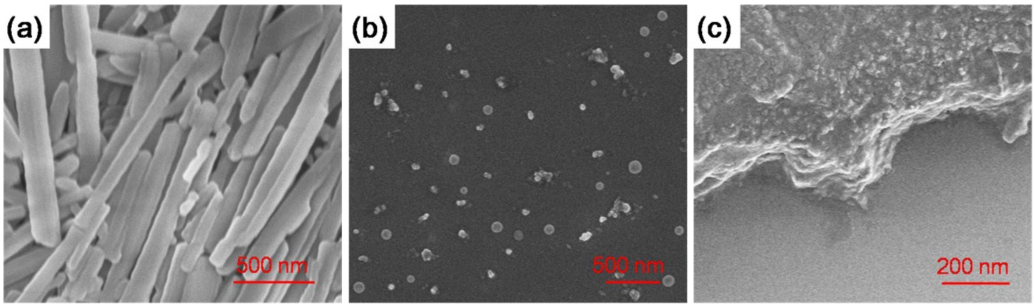

Fig. S17 (a) SEM image of ***Z*-G** (1.00 mM) in water; (b) SEM image of (a) after irradiation at 387 nm for 10 h; (c) SEM image of **WP5** (2.00 mM) and ***E*-G** (~1.00 mM) in water.

10. Possible arrangemenst of molecules in different self-assemblies

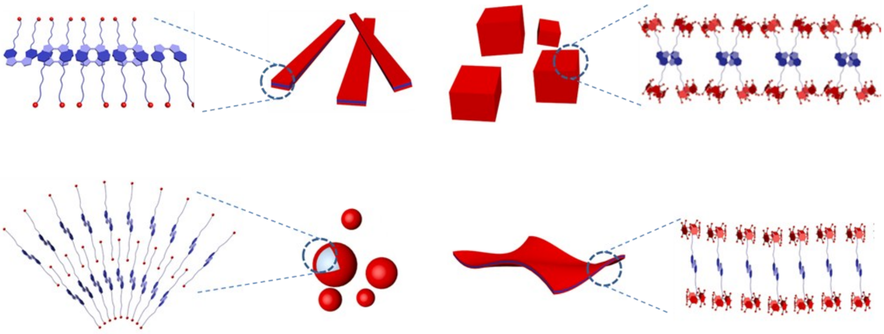

Fig. S18 Possible arrangements of molecules in different self-assemblies.

11. References:

S1 (a) T. Ogoshi, S. Kanai, S. Fujinami, T. A. Yamagishi and Y. Nakamoto, *J. Am. Chem. Soc.,* 2008, **130**, 5022–5023; (b) G. Yu, M. Xue, Z. Zhang, J. Li, C. Han and F. Huang, *J. Am. Chem. Soc.,* 2012, **134**, 13248–13251.